

Enhanced conductivity in ionic conductor-insulator composites: numerical models in two and three dimensions

G. Albinet^{1,a}, J.M. Debierre¹, P. Knauth², C. Lambert¹, and L. Raymond¹

¹ L2MP^b - Universités d'Aix-Marseille I&III, Centre Universitaire de St Jérôme, Service 142, 13397 Marseille Cedex 20, France

² MADIREL, CNRS - Université Aix-Marseille I, 3 Place Victor Hugo, 13331 Marseille Cedex 3, France

Received 10 April 2001

Abstract. We describe a two-dimensional (2D) and a three-dimensional (3D) percolation model for ionic conductor-insulator composites such as copper(I) bromide-titanium dioxide (CuBr-TiO₂) or lithium iodide-alumina (LiI-Al₂O₃). These composites present an enhanced conductivity closely related to the insulator concentration. This effect is explained by the formation of highly conducting space charge regions near the phase boundaries which are represented by good conductor bonds. Our numerical model takes into account grain size and correlation effects. The dimension has a leading role for the conduction properties. In the 2D case, the good conductor bonds do not percolate, whatever the insulator concentration, and the maximum conductivity of the composite samples is of the same order as that of the ionic conductor grains. The behavior of the system is very different in the 3D case where, for a large domain of composition, the good conductors percolate through the regions between the conductor grains. For the CuBr-TiO₂ composites the conductivity *versus* composition curve is bell-shaped. Conversely, in the LiI-Al₂O₃ system, a linear relation between the conductivity and the insulator volume fraction is obtained in the experiments. Our model gives a plausible interpretation of the conductivity in both systems.

PACS. 66.10.Ed Ionic conduction – 66.30.Dn Theory of diffusion and ionic conduction in solids

1 Introduction

A number of applications of solid ionic conductors have been developed recently, including high performance batteries and fuel cells, chemical sensors, electrochromic displays [1].

In comparison with conventional liquid electrolytes, solid electrolytes offer several advantages such as the absence of leakages and long storage lives. Furthermore, miniaturisation is possible because solids can be shaped to thin films or nano-structured materials [2]. The main limitation to their use is the low conductivity of most solid ionic conductors at room temperature. A strategy to enhance the conductivity is to prepare a composite by mixing the conductor with another material. This enhancement effect, first observed for LiI-Al₂O₃ [3], has been found subsequently in several other systems [4]. The interfaces play a major role in the conductivity enhancement, especially at moderate temperature. Experimentally, for non-metallic composites, the conductivity can be enhanced by a factor near 50.

In practice, it is of primary interest to optimize the enhancement effects by choosing the appropriate composition for the samples. To guide this choice, the dependence

of the conductivity on the composition should be systematically studied. To our knowledge, the original work of Liang remains the most complete experimental study of the conductivity over an extended range of composition [3]. However it is probable that these experiments have been biased by presence of water (molecules adsorbed on alumina surfaces) because LiI is very hygroscopic [5]. In the following we will give a plausible interpretation of the linear variation of the conductivity with the insulator proportion obtained by Liang [3].

To avoid the experimental problems related to water absorption, we have chosen to work on another type of composite, CuBr-TiO₂, in which majority charge carriers are Cu⁺ ions.

We now describe the experimental procedure shortly because we essentially focus in this work on the numerical results given by 2D and 3D models. The titanium dioxide particles have a well defined purity and grain size. The size of the CuBr grains is distributed around an average value of 5 μm but we have also done experiments with smaller granulometry [6]. The intergranular regions have an average thickness of about 0.4 μm . Impedance spectroscopy measurements were performed at frequencies ranging from 10⁻¹ Hz to 10⁵ Hz, between ambient temperature and 625 K. The measuring device and method of operation were described previously in detail [7]. The

^a e-mail: gilbert.albinet@up.univ-mrs.fr

^b UMR 6137, CNRS

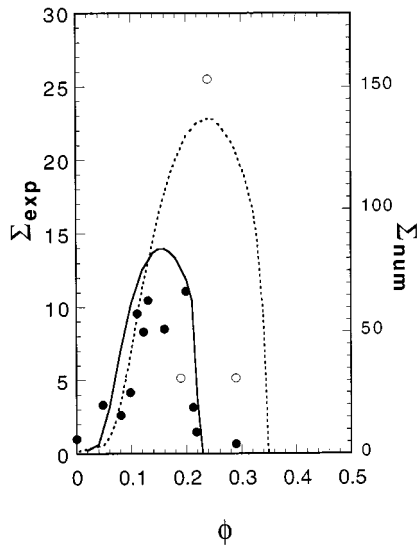


Fig. 1. Bell-shaped curves of the reduced electrical conductivity of composites *versus* volume fraction of titanium dioxide at 400 K. Experimental data differ by the grain size of ionic conductor: dark circles for 5 μm and empty circles for 3 μm . Numerical results are represented by the solid (dashed) line for $L = 25$ ($L = 15$).

conductivity is determined in a Nyquist plot from the intersection of the bulk impedance curve with the real axis. Figure 1 shows the variation of the conductivity at 400 K, as a function of the TiO_2 volume fraction, ϕ . The experimental data are normalized by the conductivity measured for pure polycrystalline CuBr, $3 \times 10^{-4} (\Omega\text{m})^{-1}$ [8]. For this bell-shaped curve, a distinct increase of conductivity is observed for ϕ higher than about 0.05, with a broad maximum, $\Sigma_{\text{max}} \simeq 10$, around $\phi = 0.15$. The conductivity drops sharply when ϕ is higher than 0.2.

The increase of conductivity can be explained [9] by the formation of space charge regions near the grain interfaces; at equilibrium, there exists a concentration profile of mobile charge carriers. Maier proposed a model predicting a linear variation of the conductivity with the composition for intermediate insulator concentrations. However, one must be cautious not to extend these predictions out of their validity domain.

For composites with an insulating oxide, the conductivity should reach a maximum and then decrease, as larger and larger amounts of the insulating material are added. Bunde *et al.* [10] have introduced a percolation model which gives a bell-shaped curve for the conductivity. In their model, insulating and conducting grains of equal size are randomly distributed on a lattice and enhanced conductivity is imposed at the interfaces between the two phases. However, in the experiments, the insulator grains are usually much smaller than the conductor grains and tend to form a layer around the latter because of the chemical affinity between both phases. These size effects and phase interactions should thus necessarily be included

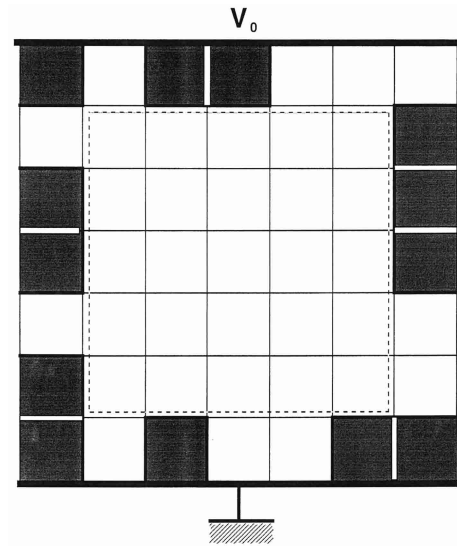


Fig. 2. Schema of the 2D random binary network, with $L = 7$ and $N_c = 1$. The white squares are conductor, the grey ones are insulator. A standard full line corresponds to a conductor bond, a bold dark line to a good conductor bond and a bold white line to an insulating bond. The dashed line limits the conductor cluster of size $L - 2$ and the exterior crown represents the space charge region, filled either with insulator (probability p) or with conductor (probability $(1-p)$). An intensity is injected at the top electrode, at potential V_0 . The bottom electrode is grounded.

in a generic model for the ionic conductor-insulator composites.

The aim of this work is to compare the numerical results obtained with 2D and 3D samples. It will be shown that the dimensionality has a drastic effect on the conduction properties of the sample and, more precisely, that the 2D models are not relevant for the experiments. In particular, the good conductor bonds do not percolate in the 2D case whereas percolation does occur through the thin inter-grain volume in 3D.

2 The two-dimensional model

We have introduced a generic model for the dispersed ionic composites [11] defined on a simple square lattice with unit cell length a . The lattice is divided into large square cells of lateral size La . The core of one cell, *i.e.*, the central part of size $(L - 2)a$ represents the bulk of a conducting grain and the external layer of thickness a belongs to the intergranular region (see Fig. 2). The $(L - 2)^2$ unit squares of size a in the inner shell are filled with conductor. The outer shell contains $N_b = L^2 - (L - 2)^2$ unit cubes and each of them is occupied either by a conductor with probability $p = (L^2/N_b)\phi = (L^2/4(L - 1))\phi$, or by an insulator with probability $1 - p$. Here ϕ is the volume fraction of conductor in the sample.

In 2D, each node α is the common corner of 4 squares and each bond is shared by 2 adjacent squares. Then three

types of bonds are defined, according to the nature of the squares. When the two adjacent squares are conductors, the central bond is set to normal conductor with a conductance G_n . Conversely, when the two squares are insulators, the central bond is set to insulator with a conductance G_i . If one square is conductor and the adjacent one insulator, then the bond between them is set to good conductor with a conductance G_g , where $G_g \gg G_n$ accounts for the enhanced conduction in the interfacial region.

A sample contains $N_c \times N_c$ cells and thus $(N_c L)^2$ unit squares. In order to limit the finite size effects, periodic boundary conditions are implemented in the transversal direction, the longitudinal direction being that of the injected current, *i.e.* the direction perpendicular to the two electrodes. It is worth noting that, in the limit $L \rightarrow 1$, the model introduced by Bunde *et al.* [10] is recovered. However, confinement of good conductor paths in narrow regions is not included in their limit, whereas it plays a fundamental role in the experiments as well as in our model when $L > 1$.

To compute the conductivity of a sample, we have to solve the system of Kirchhoff equations,

$$I_\alpha = \sum_{\beta} G_{\alpha\beta}(V_\alpha - V_\beta) \quad (1)$$

where I_α is the current flowing through the node α . The sum runs over the four nodes which are first neighbors of node α . The conductance of the bond between nodes α and β is denoted $G_{\alpha\beta}$ and V_α is the potential at node α . Two linear electrodes are placed at the top and the bottom of the sample. The top electrode is represented by a linear array of bonds of conductance G_n . The node intensities must be provided as the initial conditions. We set the total source current to unity, so that an intensity $(N_c L)^{-1}$ flows through each node of the top electrode. The total current is collected by the bottom electrode which is grounded ($V = 0$). In order to calculate the potentials, we invert the conductance matrix, using a sparse matrix resolution method [12]. The overall conductivity, Σ , is the conductance normalized to one bond. It is given by a sum over the first-neighbor pairs of nodes. The 2D conductivity and the conductance are measured by the same number,

$$\Sigma^{-1} = \sum_{\langle\alpha,\beta\rangle} G_{\alpha\beta}(V_\alpha - V_\beta)^2. \quad (2)$$

We first studied the percolation of the g -bonds (bonds of good conductance G_g) through a square lattice with $L = 25$ and N_c varying from 1 to 3. We observed that the percolation threshold ϕ_c was not reachable but, due to the finite size of the system, the g -bond percolation probability is not exactly zero for ϕ close enough to ϕ_c . For a given ϕ , this probability decreases when the sample size increases. So one can expect the sample conductance to be of the order of G_n .

Figure 3 gives the conductivity $\Sigma(\phi)$ versus the composition ϕ for three sizes ($L = 25$ and $N_c = 1, 2, 3$) and for different G_g/G_n ratios. We trivially recover $\Sigma(0) = 1$, and $\Sigma(1) = 0$. Σ reaches a maximum Σ_{\max} for a given com-

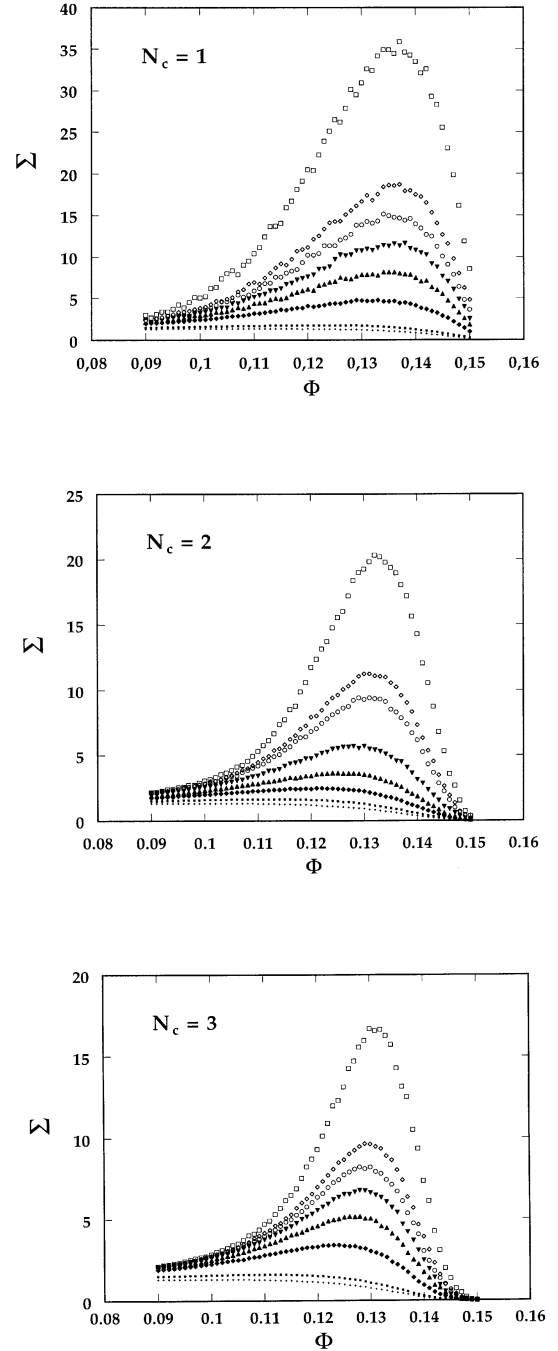


Fig. 3. The conductivity as a function of the volume fraction of insulator in the 2D case with the parameter $h = G_g/G_n$ for $L = 25$ and, respectively, $N_c = 1, 2, 3$. $h = 1000$ (\square), $h = 500$ (\diamond), $h = 400$ (\circ), $h = 300$ (\blacktriangledown), $h = 200$ (\blacktriangle), $h = 100$ (\blacklozenge), $h = 50$ (\bullet), $h = 20$ (\blacksquare) and $h = 10$ (+).

position ϕ_{\max} , which depends both on L and N_c . Some remarks ought to be done. First, it is necessary to use noticeable ($\simeq 100$) values of the ratio G_g/G_n in order to obtain a sharp maximum.

Second, we observe in Figure 1 that the conductivity decreases and ϕ_{\max} moves towards lower values, when N_c

increases. This is very clear from the curves for $N_c = 1$ and $N_c = 2$.

Let us denote p' the probability to have a g -bond in the intergranular region. For $L = 25$, a percolation test shows that the g -bonds never percolate through the larger samples: it is clear that the inter grain regions are nearly 1D so the threshold p'_c is very high. The maxima of the curves correspond to $\Delta p' N^{-1/\nu} = \text{const.}$, where $\Delta p' = |p' - p'_c|$. It is easy to show that the abscissae ϕ_{max} of the maxima decrease when N increases.

In the framework of an Effective Medium Approximation (EMA), an exact probability calculation gives for the g -bond percolation probability in a single cell ($N_c = 1$):

$$P_{\text{EMA}}(p, L) = [p(2-p)]^{L-2} \{p^2(1-p^2) + 2p(1-p) + (1-p)^2 [1 - (1-p)^{L-2}]\}^2. \quad (3)$$

In the outer shell, the unit squares are either insulator (probability $1-p$) or conductor (p).

In order to obtain g -bond percolation it is easy to see that the $N-2$ intermediate pairs of unit squares must contain one or two conductor bonds, and the probability associated to this condition is $[p(2-p)]^{(L-2)}$. Then we multiply this probability by the two identical factors associated with the two pairs of squares in contact with the electrodes.

Three cases must be taken into account for each pair (top or bottom):

i) Two insulator squares: at least one square must be out of the $L-2$ squares of the line must be an insulator. The probability is then $(1-p)^2(1-(1-p)^{L-2})$.

ii) One conductor and one insulator squares: we are sure that the g -bond percolation path exists and we have two possibilities for the localisation of the conductor (insulator) square. The probability of this mechanism is: $2p(1-p)$.

iii) The two squares are conductors. Then, at least one first neighbor cell of the insulator pair must be occupied with conductor and the associated probability is: $p^2(1-p^2)$.

For different sizes, the p values for which the maximum of P_{EMA} is obtained correspond closely to the values of p_{max} (simply related to ϕ_{max}) given by the simulations. Figure 4 shows the variations of the different bond numbers with ϕ . It is worth noting that the maximum number of good conductor bonds is reached for a ϕ value well above ϕ_{max} . In fact, as the number of insulating bonds increases too, some conductor ways are blocked. The value obtained for ϕ_{max} results from a compromise between both effects.

3 3D model for composites

3.1 Calculation of the conductivities

The method is the same as in 2D, but with a cubic array of bonds. Here each bond is the common edge of four unit cubes on the original lattice. When the four adjacent cubes are conductors, the central bond is set to normal

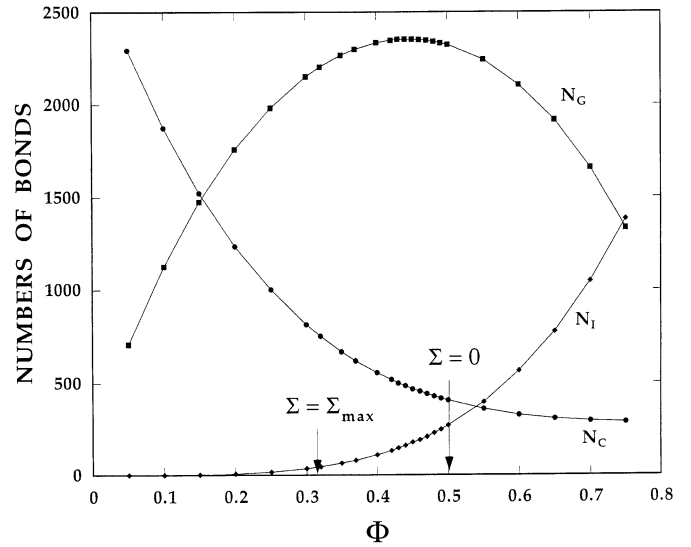


Fig. 4. Variation of the bond numbers for the three types of bonds, in the case of a cube with $L = 10$. Note that the maximum of conductivity (arrow) occurs for a value of noticeably inferior to those which corresponds to the maximum of good conductor bonds.

conductor. Conversely, when the four cubes are insulators, the central bond is set to insulator. In all the other cases, the central bond is set to good conductor.

A sample contains $(N_c L)^3$ unit cubes, or $3(N_c L)^3$ bonds, and periodic boundary conditions are implemented in the two transversal directions, the longitudinal direction being that of the injected current.

Here also we have to solve the system of Kirchhoff equations (1) in order to calculate the conductivity, but the sum runs over the six nodes which are first neighbors of a given node. The cubic array represents the f.c.c. lattice of γ -CuBr. Two planar electrodes are placed at the top and bottom faces of the sample. The top electrode is represented by a planar array of bonds of conductance G_n and the intensity $(N_c L)^{-2}$ flows through each node of the top surface.

The conductivity of the sample, normalized to one bond, reaches a value of the order G_g , much greater than in 2D. Moreover the maximum on the $\Sigma(\phi)$ curve can already be observed for small values of the ratio G_g/G_n (≈ 10) and ϕ_{max} does not vary really with N_c .

Parameters corresponding to our CuBr-TiO₂ composites were used in the simulations. From the average size of the CuBr grains and the mean thickness of the TiO₂ layers, we deduce $L = 25$. To obtain a rough estimate for the conductance ratio G_g/G_n , we used a phenomenological approach comparable to that of reference [9]. Let us schematically represent a CuBr grain by one cube of edge $\ell = 5 \mu\text{m}$. Assuming that the four lateral faces are good conductors (conductivity σ_g) and the top and bottom faces normal conductors (conductivity σ_n), the total conductance of the grain is given by $G_{\text{tot}} = 4\sigma_g(2\lambda) + \sigma_n\ell$ and the enhancement factor is $\Sigma_{\text{max}} \simeq G_{\text{tot}}/(\sigma_n\ell)$. 2λ is the thickness of the good conductor regions, where λ is

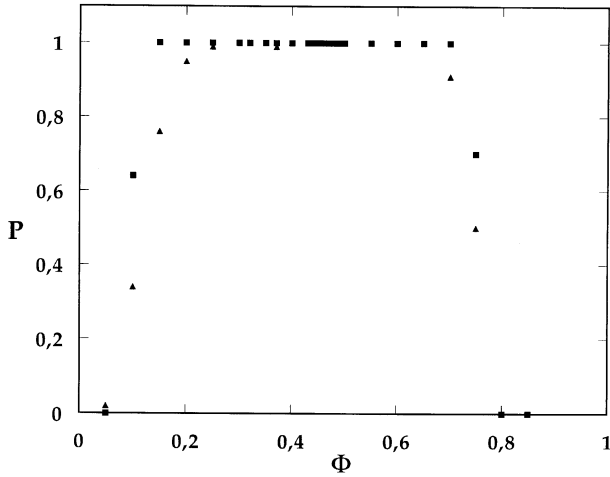


Fig. 5. The probability P of percolative structure for the good conductor bonds through 3D sample, $L = 10$, with $N_c = 1$ (\blacktriangle) and $N_c = 2$ (\blacksquare), versus the insulator proportion Φ .

the Debye length. In order to get $\Sigma_{\max} \simeq 10$ as in the experiments, one thus needs to set $G_g/G_n = \sigma_g/\sigma_n \simeq 500$ within this crude approximation. It is clear that this value is an upper bound for the actual ratio G_g/G_n and that it should only be considered as an order of magnitude. In the following, we will constantly use $G_i = 10^{-4}$, $G_n = 1$ and $G_g = 500$.

In opposition with the 2D case, the spanning probability of good conductors bonds is equal to 1 in a large domain of Φ values. Figure 5 represents this probability for a given size of the unit cube, here $L = 10$, and two values of N_c : $N_c = 1$ and 2. For the larger size, the domain of Φ values where the spanning probability is equal to 1 is larger too.

Due to the memory required to implement the matrix method, we limited the calculations to cubic lattices of size $25a$ at most. We computed Σ as a function of ϕ for cells of size $L = 5$ ($N_c = 1, 2, 3, 4$ and 5), $L = 10$ ($N_c = 1$ and 2) and $L = 25$ ($N_c = 1$). The conductivity was averaged over 100 independent samples for each value of ϕ . The corresponding data are plotted in Figure 6. For $L = 5$ and 10 , we verified that increasing N_c produced only minute changes in the $\Sigma(\phi)$ curves. We thus expect that the results obtained for one cell of size $L = 25$ are representative of a much bigger sample.

All the curves are bell-shaped and start from the value $\Sigma = 1$ for $\phi = 0$. As expected, the conductivity of the sample is seen to drop to a very low value when the outer shell is completely filled with insulators, that is for $\phi_{\text{sat}} = 1 - (1 - 2/L)^3$. For an intermediate value, ϕ_{\max} , the maximum Σ_{\max} is reached. We checked that, in the neighborhood of ϕ_{\max} , paths of good conductor bonds percolate through all the samples.

Comparing the experimental data to the numerical results for $L = 25$ (Fig. 1), we see that both values of ϕ_{\max} are comparable and that both curves have a very similar aspect. We can thus conclude that the model captures the main physical ingredients necessary for a valuable descrip-

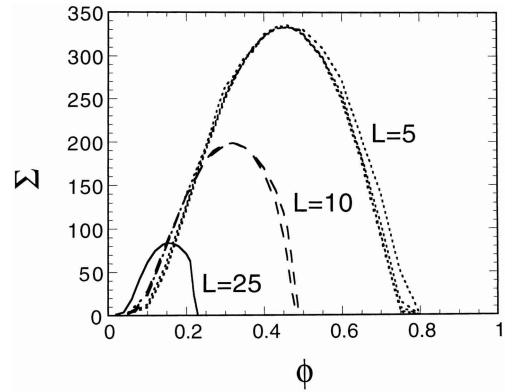


Fig. 6. The conductivity Σ of numerical samples as a function of the volume fraction of insulator ϕ . The results concern cells of size $L = 5$ ($N_c = 1, 2, 3, 4$ and 5), $L = 10$ ($N_c = 1$ and 2) and $L = 25$ ($N_c = 1$).

tion of the conductor-insulator composites. For a smaller mean size of the grains, corresponding to $L = 15$ in the model, the experimental results verify the hypothesis expressed from numerical results: the maximum of the conductivity moves towards high insulator volume fractions. This shift is easily predicted by a simple geometrical reasoning. As can be seen from Figure 1, both ϕ_{\max} and Σ_{\max} increase when L decreases. Thus the enhancement factor should increase significantly, when the size of the ionic conductor grains is decreased. In order to test these predictions we performed additional experiments with powders of different granulometries. This result is of practical importance, especially for nanostructured materials.

In addition, density measurements show that the experimental samples contain about five volume percent of voids. These voids are spread on the conductor surface and interrupt locally the conduction paths with enhanced conductivity. We verified that incorporating voids in the model samples decreased Σ_{\max} as expected. For all these reasons, varying the ratio G_g/G_n to obtain a fully quantitative agreement between the numerical and experimental results, although quite possible, would be meaningless.

Finally, samples have been generated with several square sizes with imposed proportions. In fact the simulations have been done with two types of cells, say $L_1 = L$ and $L_2 = 2L$. The cells cannot overlap and there is no void in the sample. In practice, we first impose the number N_2 of large cell, which are distributed randomly. Then the sample is filled with N_1 small cells.

A lattice $25 \times 25 \times 25$ is considered where $N_2 = 0, 1, 2, 3, 4, 5, 6, 7, 8$ cells of size $L_2 = 10$ are placed randomly. The detailed results are presented in [13].

In every case the conductivity corresponds to the mean size of the squares filling the lattice. This result is important because the grain size of the experimental samples is not mono-disperse and our simple model, with only one size for the ionic conductor grains seems to be very coarse. In fact, in the 2D case, it is the length of the phase boundaries (the area in the 3D case) which is the prominent parameter.

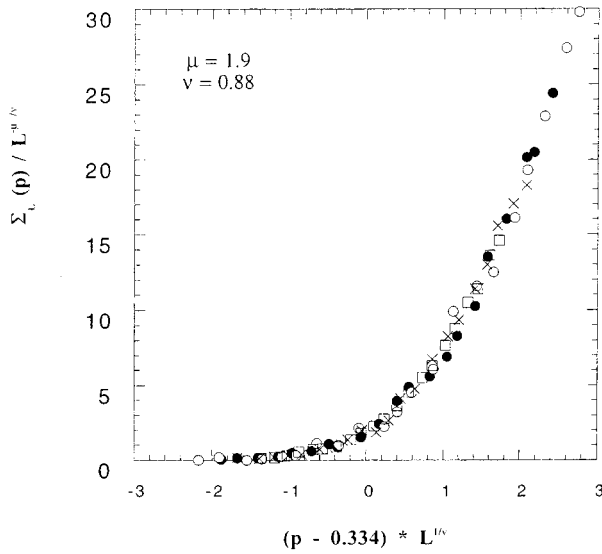


Fig. 7. Universal curve for the conductivity *versus* p' , obtained with $L = 3$ and four sizes: \square $N_c = 7$, \times $N_c = 8$, \bullet $N_c = 9$, \circ $N_c = 10$.

3.2 Self-similar properties

Let us denote N_g the number of good bonds in a given sample, the probability to find a g -bond is

$$p' = \langle N_g \rangle / 3(N_c L)^3 \quad (4)$$

where the brackets $\langle N_g \rangle$ represents the mean value of N_g over the samples. Clearly, it is impossible to impose a value of N_g which must be calculated for each sample. Then the results are sorted out in function of N_g , *i.e.* of p' .

Near the percolation threshold, the conductivity should obey a scaling law related to the size of the sample $N = L N_c$ and to the deviation $\Delta p'$ from p'_c .

$$\Sigma \simeq \sigma_g N^{-\mu/\nu} F(\Delta p' N^{1/\nu}) \quad (5)$$

where μ and ν are the regular critical exponents respectively associated with the conductivity and the correlation length in regular percolation. F is the universality function which characterizes the critical phenomena. The simulations have been done with $L = 3$ and $N_c = 1$ to 10. For given N and $\Delta p'$, the mean values are obtained from $27 \times 10^5 / N_c$ samples. We estimate the threshold probability to $p'_c = 0.334 \pm 0.001$ and the best method to obtain the critical exponent μ and ν consists in the plot of the universal curve $\Sigma N^{\mu/\nu}$ *versus* $\Delta p' N^{1/\nu}$ (see for example [14]). The best fit is obtained for $\nu \simeq 0.88$ and $\mu \simeq 2.00$, as represented in Figure 7. These values compare very well with the exponents obtained from 3D pure disordered samples, with two species only. This result is not surprising because, with $L = 3$, the samples generated are close to the disordered case.

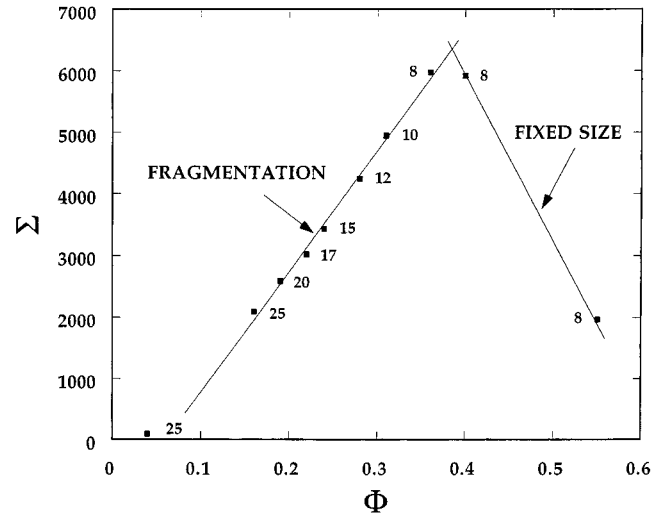


Fig. 8. Normalized electrical conductivity Σ/Σ_0 of LiI- Al_2O_3 composites *versus* the volume fraction of alumina ϕ .

4 3D model of a reactive system

Our theory allows us to predict some astonishing properties of the insulator-conductor mixtures. For instance that the conductivity of a sample increases when the ionic conductor grains are more finely divided [11]. Such an effect was demonstrated in the case of epitaxial heterolayers $\text{CaF}_2/\text{BaF}_2$ [15]. It also allows to understand the particular behavior of some experimental systems. For instance, in the initial experiments on the system LiI- Al_2O_3 , Liang [3] obtained experimentally a nearly linear variation of the conductivity with the composition, until a maximum was reached and the conductivity decreased when more insulator was added. Maier's [9] theory is in agreement with this result, but it does not cover the whole composition domain studied by Liang. In fact, alumina has a much higher basicity than titania. It carries water molecules and wets the ionic conductor LiI which is a hygroscopic compound. One can assume that smaller grains are formed when the alumina proportion increases. The simplest relation between the mean grain size d and the insulator volume fraction ϕ is: $\phi = K/d$. Figure 8 shows the results obtained when we assume this simple relation. The constant factor K was chosen in order to recover Liang's experimental value for Σ_{max} . In this model, the maximum conductivity corresponds to the minimum grain size of LiI that can be reached corresponding *e.g.* to the distance between two crystal defects (dislocations, stacking faults, ...). The experimental results are in good qualitative agreement with the simulations. This hypothesis can also explain the significant difference between the results obtained with CuBr-alumina and CuBr-titania composites. In the latter case, interfacial interactions are smaller and an imperfect wetting is observed, so that the mean grain size of CuBr is approximately constant whatever the fraction of titania. In CuBr-alumina the interactions

are larger so that a variation of grain sizes of CuBr is observed, resulting in a linear variation of conductivity with alumina proportion [16].

5 Conclusion

The conductivity enhancement observed in certain ionic conductor-insulator composites can be simulated using the outlined realistic physical model, based on the existence of highly conducting regions confined near the phase boundaries. The different grain sizes of insulator and ionic conductor and the phase interactions are taken into account. Bond percolation is only observed in 3D systems, but never in two dimensions. The critical exponents are close to the regular case.

The simulations predict a strong enhancement of conductivity with reduction of the ionic conductor particle size. This is verified for the CuBr-TiO₂ system. Furthermore, the case of a variable particle size, resulting from strong interactions with the second phase, is also at least qualitatively simulated, exemplified by the system LiI-Al₂O₃. The model can be used as a guide for experimentation and to predict the electrical conductivity of this type of composite materials.

References

1. See, *e.g.*, *Solid State Electrochemistry*, edited by P.G. Bruce (University Press, Cambridge 1995).
2. N.J. Dudney, B.J. Neudecker, *Curr. Opin. Sol. State Mat. Sc.* **4**, 479, (1999); H.L. Tuller, *Sol. State Ionics* **131**, 143 (2000).
3. C.C. Liang, *J. Electrochem. Soc.* **120**, 1289 (1973).
4. U. Hariharan, J. Maier, *J. Electrochem. Soc.* **142**, 3469 (1995); M. Nagai, T. Nishino, *Sol. State Ionics* **70/71**, 96 (1994); M. Nagai, T. Nishino, *J. Amer. Ceram. Soc.* **76**, 1057 (1993); J. Maier, B. Reichert, *Ber. Bunsenges. Phys. Chem.* **90**, 666 (1986); J. Maier, *Mat. Res. Bull.* **20**, 383 (1985); K. Shahi, J.B. Wagner, *J. Electrochem. Soc.* **128**, 6 (1981); T. Jow, J.B. Wagner, *J. Electrochem. Soc.* **126**, 1963 (1979). U. Lauer, J. Maier, *J. Electrochem. Soc.* **139**, 1472 (1992); P. Knauth, *J. Electroceramics* **5**, 111 (2000).
5. S. Pack, B. Owens, J.B. Wagner, *J. Electrochem. Soc.* **127**, 2177 (1980).
6. P. Knauth, G. Albinet, J.-M. Debierre, *Ber. Bunsenges. Phys. Chem.* **102**, (1998).
7. S. Villain, J. Cabané, D. Roux, L. Roussel, P. Knauth, *Sol. State Ionics* **76**, 229 (1995); A. Becquart, F. Cabané, P. Knauth, *J. Electroceramics* **2**, 173 (1997).
8. S. Villain, M.A. Desvals, G. Clugnet, P. Knauth, *Sol. State Ionics* **83**, 191 (1996).
9. J. Maier, *J. Phys. Chem. Solids* **46**, 309 (1985); J. Maier, *Ber. Bunsenges. Phys. Chem.* **90**, 26 (1986); J. Mayer, *Prog. Sol. State Chem.* **23**, 171 (1995).
10. A. Bunde, W. Dietrich, E. Roman, *Phys. Rev. Lett.* **55**, 5 (1985); E. Roman, A. Bunde, W. Dietrich, *Phys. Rev. B* **34**, 3439 (1986).
11. J.-M. Debierre, P. Knauth, G. Albinet, *Appl. Phys. Lett.* **73**, 1337 (1997).
12. W.H. Press, S.A. Teukolsky, W.T. Vetterling, B.P. Flannery, *Numerical Recipes in C: the Art of Scientific Computing*, (Cambridge: Cambridge University Press, 1992), p. 71.
13. C. Lambert, L. Memoli, J.M. Debierre, P. Knauth, G. Albinet, *Ionics* **5**, 200 (1999).
14. J.P. Straley, *J. Phys. C* **9**, 783 (1976); J.P. Straley, *Phys. Rev. B* **15**, 5733 (1977).
15. N. Sata, K. Eberman, K. Eberl, J. Maier, *Nature* **408**, 946, (2000).
16. M.A. Desvals, P. Knauth, *J. Phys. Chem. Sol.* **58**, 319 (1997).